ACS Catalysis

RESEARCH ARTICLE

pubs.acs.org/acscatalysis

Methyl Formate Pathway in Methanol Steam Reforming on Copper: Density Functional Calculations

Sen Lin,[†,§] Daiqian Xie,[*,†] and Hua Guo[*,‡]

[†]Institute of Theoretical and Computational Chemistry, Key Laboratory of Mesoscopic Chemistry, School of Chemistry and Chemical Engineering, Nanjing University, Nanjing 210093, China

[‡]Department of Chemistry and Chemical Biology, University of New Mexico, Albuquerque, New Mexico 87131, United States

Supporting Information

ABSTRACT: Methyl formate has been proposed to be an intermediate in methanol steam reforming (MSR) on copper catalysts. We show here using plane-wave density functional theory that methyl formate can indeed be formed by reaction between formaldehyde and methoxyl. However, this reaction competes unfavorable with that between formaldehyde and hydroxyl, which explains why methyl formate is only observed in the absence of water. Methyl formate can be further hydrolyzed by a surface OH species to produce formic acid, which can dehydrogenate to produce CO_2. This process has a lower overall barrier than MSR, thus consistent with the experimental observation that the steam reforming of methyl formate is faster than MSR. However, this hydrolysis process might have difficulties competing with desorption of methyl formate, which has a small adsorption energy. Our theoretical model, which is consistent with all experimental observations related to methyl formate in MSR, thus assigns a minor role for the methyl formate pathway.

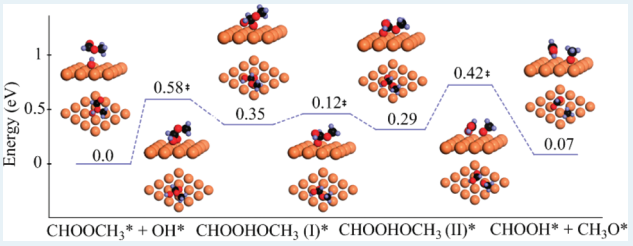

KEYWORDS: methanol steam reforming, methyl formate, DFT, Cu(111)

I. INTRODUCTION

Polymer electrolyte membrane (PEM) fuel cells represent an energy efficient and environmentally friendly solution to many of our energy problems, particularly for mobile applications. However, its popularization has been fraught with difficulties, particularly in storing and transporting of the hydrogen fuel. To circumvent this problem, it has been suggested that hydrogen carriers, such as methanol (CH_3OH),[1] can be used to generate H_2 in situ. A promising scheme is methanol steam reforming (MSR), which provides high purity hydrogen gas to fuel cells on demand.[2−5] The MSR-based solution has a number of advantages. For example, the liquid nature of methanol allows leveraging the existing infrastructure in fuel storage and dispensing. The technology for large scale production of methanol from other industrial feedstocks, such as natural gas, oil, and even biomass, is well established. Finally, it is a relatively clean fuel, with essentially no sulfur, a large H/C ratio, and biodegradable.

Although the MSR reaction,

$$CH_3OH + H_2O \rightarrow 3H_2 + CO_2 \quad \Delta H^0 = 49.6\ \text{kJ/mol}$$

appears deceptively simple, its mechanism is far from elucidated. The traditional catalyst for MSR is copper dispersed on oxide support, which is highly selective toward CO_2 over CO.[2,4,5] This is important as the CO byproduct poisons the PEM anode and generates pollution. Extensive experimental evidence indicated that the rate of MSR is limited by the dehydrogenation of methoxyl (CH_3O^*),[6−9] which can be produced by cleavage of the O−H bond of methanol. Three putative mechanisms have been proposed for MSR on copper catalysts, all initiated with the dehydrogenation of methanol and methoxyl.[4,5] The earlier proposal envisages methanol decomposition to CO*, which is then converted to CO_2 via the water-gas shift (WGS) reaction ($CO + H_2O \rightarrow H_2 + CO_2$).[2] However, the relevance of this decomposition/shift pathway is now discounted by most researchers,[4] since methanol is found to inhibit WGS.[6,10,11]

The more probable mechanisms are based on reactions of formaldehyde (CH_2O^*) with other species. Formaldehyde is produced by dehydrogenation of methoxyl (CH_3O^*). Its intermediacy in MSR is well established since formaldehyde has been detected in MSR[11] and in decomposition reaction of CH_3OH on Cu.[12−14] Furthermore, the same CO_2 and H_2 products are produced when formaldehyde is fed with steam under MSR conditions.[11] Nevertheless, the subsequent steps leading to the H_2 and CO_2 products are much less understood than the initial dehydrogenation reactions, and several proposals have been advanced.

One such proposal suggests that CH_2O^* reacts with surface OH* or O* species, which produce intermediates such as formic acid (CHOOH*), formate (CHOO**), and dioxomethylene (CH_2OO^{**}).[10] Dehydrogenation of these species leads eventually to CO_2 and H_2. We will refer this as the formate mechanism. Alternatively, it has been suggested that methyl formate ($CHOOCH_3^*$) might be involved,[6,7,11] as it has been

Received: June 12, 2011
Revised: July 26, 2011
Published: August 15, 2011

Table 1. Adsorption Energies and Geometric Parameters for Various Pertinent Species in the Methyl Formate Pathway on Cu(111)[a]

species	adsorption configuration	$D_{Cu\text{-}A}$ (Å)	adsorption energy (eV)	bonding details: bond	bonding details: length (Å)
O	fcc/Hcp through O	1.90	−4.94 (−4.86)/ −4.94 (−4.87)		
OH	fcc through O	2.03	−3.21 (−3.12)	O−H	0.97
CH_3	hcp through C	2.24	−1.50 (−1.42)	C−H	1.11
		2.23			
		2.23			
CH_2OOCH_3	fcc through carbonyl O	2.06	−2.18 (−2.03)	C_1−O	1.43/1.40
		2.04		C_2−O	1.43
		2.04		C_1−H	1.10/1.11
				C_2−H	1.10/1.11
$CHOOCH_3$	top through carbonyl O	2.64	−0.07 (−0.06)	C_1=O	1.22
				C_1−O	1.34
				C_2−O	1.45
				C_1−H	1.10/1.11
$CHOOCH_2$	top−top through methylene C and carbonyl O	2.03	−0.93 (−0.84)	C_1=O	1.24
		2.17		C_1−O	1.32
				C_2−O	1.47
				C_1−H	1.10
				C_2−H	1.10/1.11
$CHOOOCH_3$	bridge−bridge through two terminal Os	2.05	−4.22 (−4.12)	C_1−O	1.40/1.41/1.42
		2.05		C_2−O	1.42
		2.01		C_1−H	1.10
		1.98		C_2−H	1.10/1.11
$CHOOHOCH_3$(I)	bridge−top through two terminal Os	2.04	−2.51 (−2.39)	C_1−O	1.36/1.41/1.45
		2.05		C_2−O	1.43
		2.33		C_1−H	1.11
				C_2−H	1.10
				O−H	0.98
$CHOOHOCH_3$(II)	bridge−top through two terminal Os	2.04	−2.58 (−2.45)	C_1−O	1.36/1.40/1.47
		2.04		C_2−O	1.44
		2.18		C_1−H	1.11
				C_2−H	1.10
				O−H	0.98

[a] The numbers in parentheses are corrected by ZPE.

detected under certain conditions. For example, methyl formate was found in methanol decomposition over Cu in the absence or at low concentrations of water.[10,14−16] However, its production diminishes at lower temperatures.[10] An interesting observation is that the steam reforming of methyl formate on copper is about 30 times faster than MSR.[15] A more recent study found $CH_3{}^{18}OH$ as a product in MSR with $CH_3{}^{16}OH$ and $H_2{}^{18}O$, and it was concluded that MSR proceeds via the methyl formate mechanism.[17] However, as we discuss below, this conclusion is premature.

Methyl formate is weakly adsorbed on Cu thanks to its closed-shell electronic structure.[18] There have been several attempts to detect this species on catalyst surfaces in situ during MSR, but with little success. The diffuse reflectance infrared Fourier transform spectroscopy (DRIFT) experiments by Peppley et al.[7] and more recently by Frank et al.[9] found no methyl formate on the catalyst surface under normal MSR conditions. Interestingly, the latter did detect signatures of methoxyl, hydroxyl, and formate, which support the formate mechanism. However, these observations could not rule out the intermediacy of methyl formate.[9]

Given the experimental difficulties, theoretical studies are highly desired because they can provide complementary, and sometimes more detailed, information about reaction mechanisms.[19] Earlier density functional theory (DFT) calculations have focused on the decomposition of CH_3OH^* and H_2O^* on copper surfaces in

dx.doi.org/10.1021/cs200311t |ACS Catal. 2011, 1, 1263–1271

MSR.[20−29] More recently, efforts have been made to understand the more complex later reaction network.[29−31] It has been realized that the reaction of the formaldehyde intermediate with hydroxyl is a key step in producing the $CO_2 + H_2$ product. For example, our recent work has demonstrated that this reaction has a very small (0.11 eV) barrier and a relatively large (−0.64 eV) exothermicity.[31] Very similar results have been obtained independently by Gu and Li.[29] As a result, the formation of CH_2OOH^* on the Cu surface can compete effectively with the desorption of CH_2O^* or its further dehydrogenation which has a barrier of 0.65 eV.[20] We have also shown that CH_2OOH^* can react further to produce CO_2 without any higher barriers than the rate-limiting step for MSR. In addition, some of these pathways include the formate intermediate, thus consistent with the DRIFT experiment.[9]

In addition to the recent theoretical work on MSR, there are several related studies on methanol synthesis,[32−34] which is the reverse reaction of MSR. The comprehensive DFT work of Grabow and Mavrikakis has concluded that the major pathway in methanol synthesis involves formic acid, formate, and formaldehyde,[34] in agreement with our recent suggestion for the same process based on DFT studies of MSR on Cu(111).[31]

However, previous work has not addressed the involvement of methyl formate in MSR, which can in principle be formed via the reaction between CH_2O^* and CH_3O^* on the surface. Here, we present an extensive DFT study on the adsorption and reactivity of methyl formate and related species on Cu(111). These results will help us to clarify the relevance of the methyl formate pathway in MSR. This work is organized as follows. Sec. II discusses the theory and model. The calculation results are presented in Sec. III, and their implications on MSR mechanism are discussed in Sec. IV. The final conclusion is given in Sec. V.

II. THEORY

All DFT calculations were carried out using the Vienna ab initio simulation package (VASP)[35−37] with the gradient-corrected PW91 exchange-correction functional.[38] The ionic cores were described with the projector augmented-wave (PAW) method[39,40] and for valence electrons a plane-wave basis set with a cutoff of 400 eV was employed. The Brillouin zone was sampled using a 4 × 4 × 1 Monkhorst-Pack *k*-point grid[41] with Methfessel-Paxton smearing of 0.1 eV.[42] The optimized bulk lattice parameter for Cu was found to be 3.67 Å, in good agreement with the experimental value (3.62 Å).[43] Slab models for the Cu(111) surface consisted of three layers of a 3 × 3 unit cell, with the top layer allowed to relax in all calculations. A vacuum space of 14 Å was used in the *z* direction. This 3-layer model has been tested against a 4-layer model for several adsorbates, and the errors in adsorption energy are found to be only a few percent. Similar tests have also been performed for two reactions, and again, the errors in reaction barrier as well as exothermicity are within a range of a few percent.

The adsorption energy was calculated as follows: $E_{ads} = E(\text{adsorbate + surface}) - E(\text{free molecule}) - E(\text{free surface})$. The climbing image nudged elastic band (CI-NEB) method[44,45] was used to determine the reaction pathways with the energy (10^{-4} eV) and force (0.05 eV/Å) convergence criteria. Stationary points were confirmed by normal-mode analysis using a displacement of 0.02 Å and energy convergence criterion of 10^{-6} eV; and the vibrational frequencies were used to compute zero-point energy (ZPE) corrections.

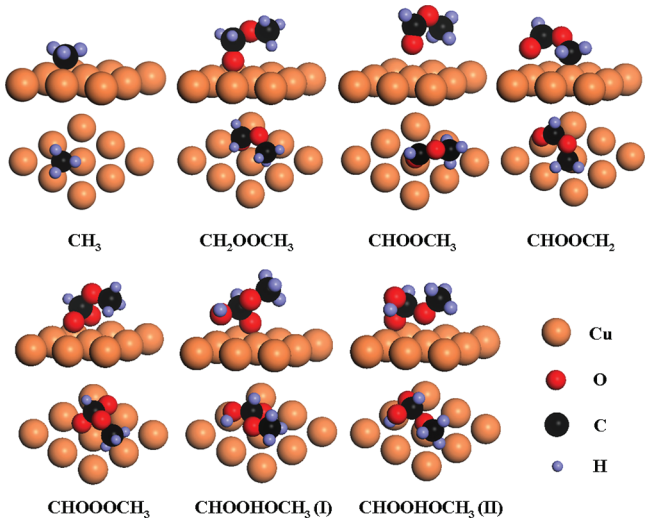

Figure 1. Adsorption geometries of several pertinent species on Cu(111).

III. RESULTS

A. Adsorption of Pertinent Species. The adsorption of pertinent species in the elementary reactions on Cu(111) discussed below has been studied. The adsorption geometries and adsorption energies of these species are listed in Table 1. The adsorption patterns of several key species are displayed in Figure 1. Except for the OH* and O* species, we will not discuss the species that have been investigated in our previous work.[31]

A-1. OH and O*.* The hydroxyl species is produced by O−H bond cleavage of H_2O^*, which is a near-thermoneutral reaction with a barrier of 1.15 eV on Cu(111).[46] There is experimental evidence that OH* is present during the MSR process,[9] but kinetic studies indicated that the rate is independent of the water partial pressure. These experimental observations seem to suggest that the OH* species is produced on copper catalyst, but the precise process is still unclear. Here, we assume that there are sufficient OH* species on Cu(111) and they react with other adsorbed species, as discussed below.

The O* species can be produced in two ways. First, it can be formed by cleaving the O−H bond in OH*, which has a very high (1.76 eV) barrier.[46] This route is probably unfeasable under MSR conditions. Alternatively, it can be formed via the disproportionation reaction ($OH^* + OH^* \rightarrow O^* + H_2O^*$), which has a relatively low (0.25 eV) barrier.[46] However, the latter process consumes OH* species. It is reasonable to assume that O* is negligible on the catalyst.

The adsorption of both OH* and O* on Cu(111) has been discussed in our earlier work.[31] Briefly, OH* adsorbs at an fcc site with an adsorption energy of −3.12 eV. It assumes a perpendicular configuration. On the other hand, the O* species adsorbs at an fcc/hcp site with an even larger adsorption energy (−4.86 eV).

A-2. CH_3.* As shown in Figure 1, methyl preferentially adsorbs at an hcp site through its carbon atom. The distances between the C atom and surface Cu atoms are 2.24, 2.23, and 2.23 Å, respectively. The adsorption energy was found to be −1.42 eV.

A-3. CH_2OOCH_3.* Similar to CH_2OOH^*,[31] this species adsorbs on Cu(111) with its carbonyl oxygen at an fcc site with methyl pointing away from the surface, as shown in Figure 1. The distances between the adsorbing O atom and the three surface

dx.doi.org/10.1021/cs200311t |ACS Catal. 2011, 1, 1263–1271

Table 2. Calculated Activation and Reaction Energies (eV) for Several Elementary Reactions on Cu(111) Studied in This Work[a]

no.	elementary reaction	activation energy $E^{\ddagger}$	exothermicity ΔE
R1	$CH_2O^* + CH_3O^* \rightarrow CH_2OOCH_3^*$	0.31 (0.30)	−0.61 (−0.47)
R2	$CH_2OOCH_3^* \rightarrow CHOOCH_3^* + H^*$	0.89 (0.70)	0.10 (−0.06)
R3	$CH_2OOCH_3^* + OH^* \rightarrow CHOOCH_3^* + H_2O^*$	1.43 (1.26)	−0.41 (−0.40)
R4-I	$CHOOCH_3^* + OH^* \rightarrow CHOO^* + CH_3OH^*$	2.05 (1.84)	−0.31 (−0.30)
R4-IIa	$CHOOCH_3^* + OH^* \rightarrow CHOOHOCH_3(I)^{**}$	0.57 (0.58)	0.29 (0.35)
R4-IIb	$CHOOHOCH_3(I)^{**} \rightarrow CHOOHOCH_3(II)^{**}$	0.13 (0.12)	−0.06 (−0.06)
R4-IIc	$CHOOHOCH_3(II)^{**} \rightarrow CHOOH^* + CH_3O^*$	0.52 (0.42)	−0.14 (−0.22)
R5-I	$CHOOCH_3^* + O^* \rightarrow CHOO^{**} + CH_3O^*$	2.13 (2.01)	−1.01 (−1.00)
R5-IIa	$CHOOCH_3^* + O^* \rightarrow CHOOOCH_3^{**}$	0.36 (0.35)	0.18 (0.19)
R5-IIb	$CHOOOCH_3^{**} \rightarrow CHOO^{**} + CH_3O^*$	0.12 (0.08)	−1.12 (−1.15)
R6	$CHOOCH_3^* \rightarrow CHOOCH_2^* + H^*$	1.62 (1.43)	0.98 (0.86)
R7	$CHOOCH_3^* \rightarrow CHOO^{**} + CH_3^*$	1.66 (1.50)	−0.41(−0.52)

[a] Entries in the parentheses are the ZPE-corrected values.

Cu atoms are 2.06, 2.04, and 2.04 Å, respectively. The C−O−C and O−C−O angles were found to be 114.55° and 112.10°, respectively. From the adsorption energy of −2.03 eV, it is clear that this species adsorbs chemically on Cu(111).

A-4. $CHOOCH_3$.* Because of its closed-shell character, methyl formate adsorbs weakly on Cu(111) with a calculated adsorption energy of −0.06 eV, which can be compared with the recent DFT value of −0.10 eV on the same surface.[34] This value is likely to be an underestimation as DFT does not describe dispersion forces very well.[47] An earlier TPD experiment showed that methyl formate desorbs from Cu(110) near 155 K,[18] which gives an adsorption energy of −0.41 eV according to the Redhead theory.[48] However, this value was determined at the monolayer coverage, which presumably included the adsorbate−adsorbate interaction.

As shown in Figure 1, methyl formate adsorbs with its carbonyl oxygen on Cu through its lone pair electrons, in agreement with experimental findings.[18,49] The distance between the carbonyl oxygen and the underlying Cu atom is 2.64 Å, which is longer than that of formic acid CHOOH*.[31] The methyl group points toward the surface with the O−C−O and C−O−C angles of 126.53° and 116.23°, respectively, while the hydrogen atom at the carbonyl carbon points upward. The three calculated O−C bonds are found to be 1.22, 1.34, and 1.45 Å, respectively.

*A-5. $CHOOCH_2$**.* Generated from dehydrogenation of $CHOOCH_3$*, this species preferentially adsorbs in a bidentate fashion with both the carbonyl O and the methylene C on the top of Cu atoms with the O−Cu and C−Cu distances of 2.17 and 2.03 Å, respectively. The calculated C−O−C and O−C−O angles are 118.42° and 126.25°, respectively. The binding energy is −0.84 eV.

*A-6. $CHOOOCH_3$**.* This is a metastable species formed as a result of the O* attack of the carbonyl carbon of methyl formate. It has a large adsorption energy (−4.12 eV), with two carboxylate oxygen moieties on bridge sites. As shown in Figure 1, the methoxyl group is nearly parallel to the surface. In addition, the three O−C−O angles are found to be 111.02°, 111.47°, 112.82°, respectively; and the C−O−C angle has a larger value of 118.90°. The adsorption geometry is very similar to that reported recently by Grabow and Mavrikakis.[34]

*A-7. $CHOOHOCH_3(I)$**.* The reaction of OH* and $CHOOCH_3$* leads to the generation of the $CHOOHOCH_3$** species which adsorbs through the hydroxyl oxygen on the top of a Cu atom (the angle of H−O−Cu is calculated to be 111.81°) and another carboxylate oxygen atom at the bridge site, as shown in Figure 1. The binding energy is calculated to be −2.39 eV, indicating strong adsorption. The distance between hydroxyl oxygen and Cu atom is found to be 2.23 Å, and the lengths of Cu−O (bridge site) are 2.04 and 2.05 Å, respectively. Slightly different from the CHO $OOCH_3$** species, the three O−C−O angles become 110.61°, 104.16°, and 113.46°, respectively, and the C−O−C angle is found to be 113.42°.

*A-8. $CHOOHOCH_3(II)$**.* This species, which was identified by our NEB calculations of the decomposition of $CHOOHOCH_3$-(I)**, is 0.06 eV slightly more stable than $CHOOHOCH_3(I)$** on Cu(111). Different from $CHOOHOCH_3(I)$**, it interacts with Cu(111) surface through methoxyl O on the top of Cu atom and a carboxylate oxygen at the bridge site. Furthermore, the three O−C−O angles are calculated to be 113.32°, 110.25°, and 106.62°, respectively, and the C−O−C angle extends to 114.57°. In addition, this species has the H of the hydroxyl group pointing to the surface, as shown in Figure 1.

B. Reactions. The barriers and exothermicities for several elementary reactions on Cu(111) are listed in Table 2, with the ZPE-corrected values in parentheses. The geometries of the initial states (ISs), transition states (TSs), and final states (FSs) for all reactions except R4-II and R5-II are displayed in Figure 2. In addition to the reactions listed here, we have also performed NEB calculations for the dehydrogenation of CH_3OH* and CH_3O* on Cu(111), and our results are very close to the most recent DFT study.[29]

It is important to note that all reactions studied here are assumed to proceed with only those species involved in the reaction. In reality, however, many species coadsorb on the catalyst surface, and they might influence the reaction barrier significantly. To model such processes, it is necessary to know the populations of various species and their adsorption sites, which require detailed kinetic simulations. In this work, we will focus on the chemical steps without other coadsorbed species, but with a caveat that the calculated barrier heights and other properties may be altered by the presence of other species.

B-1. R1: $CH_2O^* + CH_3O^* \rightarrow CH_2OOCH_3$.* This reaction is very similar to that between formaldehyde and hydroxyl. The methoxyl adsorbs at an fcc site while the formaldehyde is loosely bound on Cu(111). The product CH_2OOCH_3* also adsorbs at the fcc site. The barrier of 0.30 eV is relatively low, and the reaction is exothermic (ΔE = −0.47 eV). As discussed below, this

dx.doi.org/10.1021/cs200311t |ACS Catal. 2011, 1, 1263–1271

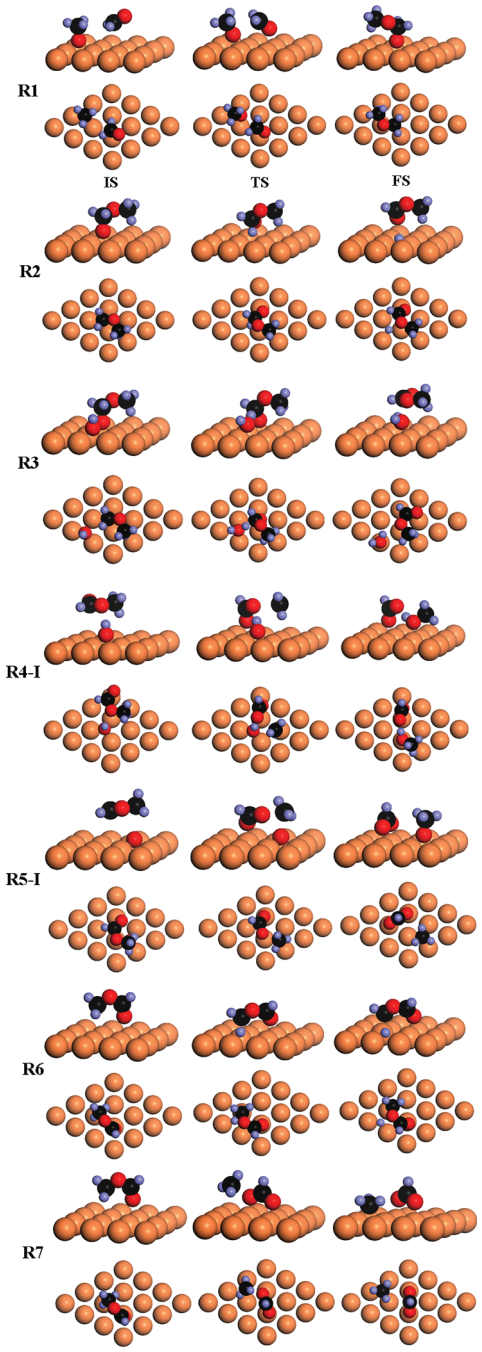

Figure 2. Side and top views of the initial states (IS), transition states (TS), and final states (FS) for several elementary reactions listed in Table 2.

is important as the reaction needs to compete with the desorption of formaldehyde.

B-2. R2: $CH_2OOCH_3^* \rightarrow CHOOCH_3^* + H^*$. The dehydrogenation of $CH_2OOCH_3^*$ produces $CHOOCH_3^*$, which weakly interacts with the Cu surface through its carbonyl O atom. The length of breaking C−H bond is 1.48 Å at the transition state. After dissociation, the H atom adsorbs at an hcp site. This nearly thermoneutral ($\Delta E = -0.06$ eV) reaction has a barrier of 0.70 eV.

B-3. R3: $CH_2OOCH_3^* + OH^* \rightarrow CHOOCH_3^* + H_2O^*$. Like R2, this reaction produces methyl formate, but via hydrogen abstraction by OH*. Judging from the barrier height (1.26 eV), this reaction route is much less feasible than R2. The methyl formate produced by this reaction is weakly bound by the surface and H_2O^* coadsorbs nearby on a top site.

B-4. R4-I: $CHOOCH_3^* + OH^* \rightarrow CHOO^* + CH_3OH^*$. The hydrolysis of methyl formate by OH* can happen in two ways. First, we consider the reaction via OH* attacking the methyl carbon, denoted as R4-I. In the initial state, $CHOOCH_3^*$ is parallel on the surface, and OH* adsorbs at an fcc site. The attack cleaves the bond between the CH_3 group and the remainder of methyl formate, replacing it with a bond between OH* and the CH_3 moiety. There is only one transition state, and the ZPE-corrected barrier is calculated to be 1.84 eV, which indicates that this reaction is very difficult to occur. In the product state, CH_3OH^* is formed at the top site and CHOO* adsorbs at a bridge site in a unidentate fashion. As shown in Figure 2, the H atom of CH_3OH^* forms a hydrogen bond with a carbonyl oxygen of CHOO*.

B-5. R4-II: $CHOOCH_3^* + OH^* \rightarrow CHOOH^* + CH_3O^*$. Next, we consider the OH* attack at the carbonyl carbon of methyl formate. This reaction is found to be stepwise, involving the $CHOOHOCH_3^{**}$ intermediate. The first step, or R4-IIa, features a barrier of 0.58 eV, and the product of this step, $CHOOHOCH_3(I)^{**}$, is 0.23 eV higher than the reactant. The second step, denoted as R4-IIb, involves a change of the adsorption pattern from $CHOOHOCH_3(I)^{**}$ to $CHOOHOCH_3(II)^{**}$, which has a low barrier of 0.12 eV and is nearly thermoneutral. This step is important to reorient the adsorbate for its decomposition. Finally, the final step (R4-IIc) involves the decomposition of $CHOOHOCH_3(II)^{**}$ into CH_3O^* and CHOOH*. The barrier (0.42 eV) is lower than that of R4-IIa. After reaction, the CH_3O^* moves to an fcc site and CHOOH* interacts with Cu atom through its carbonyl O atom. In addition, this step is exothermic (−0.22 eV). The energetics for this reaction and the geometries of the stationary points are displayed in Figure 3. We emphasize that the hydroxyl reactant is in the CHOOH* product, in contrast to R4-I where the hydroxyl is in the CH_3OH^* product.

B-6. R5-I: $CHOOCH_3^* + O^* \rightarrow CHOO^{**} + CH_3O^*$. Like its reaction with OH*, methyl formate can react with the more reactive O* species with two possible schemes. The attack of O* at the methyl carbon of methyl formate (R5-I) leads to CHOO**, which adsorbs in a bidentate fashion through the two oxygen atoms at top sites, and CH_3O^*, which adsorbs at an fcc site. This reaction, like its R4-I counterpart, has a high (2.01 eV) barrier.

B-7. R5-II: $CHOOCH_3^* + O^* \rightarrow CHOO^{**} + CH_3O^*$. Similar to R4-II, this reaction is indirect and involves an intermediate, as suggested previously by Grabow and Mavrikakis.[34] The first step, R5-IIa, features the attack of O* at the carbonyl carbon of methyl formate, which leads to a metastable $CHOOOCH_3^{**}$ intermediate, with two oxygen moieties at bridge sites. The barrier for this step is relatively low (0.35 eV). At the transition state, the distance between the hydroxyl O and carbonyl C is about 1.49 Å. The $CHOOOCH_3^{**}$ intermediate decomposes in the second step (R5-IIb) to CHOO** and CH_3O^*. This step has a small (0.08 eV) barrier and a large ($\Delta E = -1.15$ eV) exothermicity. The product state is the same as that of R5-I, but the reactant O* is in CHOO*, rather than in CH_3O^* in R5-I. The energetic and geometries of stationary points are displayed in Figure 4. Our results on this reaction are similar to that reported recently by Grabow and Mavrikakis.[34]

B-8. R6: $CHOOCH_3^* \rightarrow CHOOCH_2^* + H^*$. The dehydrogenation of $CHOOCH_3^*$ to $CHOOCH_2^*$ has a high barrier (1.43 eV),

dx.doi.org/10.1021/cs200311t |ACS Catal. 2011, 1, 1263–1271

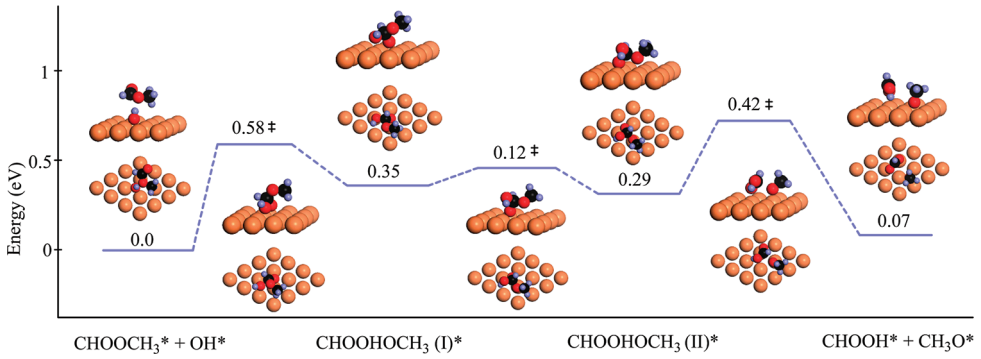

Figure 3. Energetics and geometries (top and side views) of the $CHOOCH_3^* + OH^* \rightarrow CHOOH^* + CH_3O^*$ (R4-II) reaction.

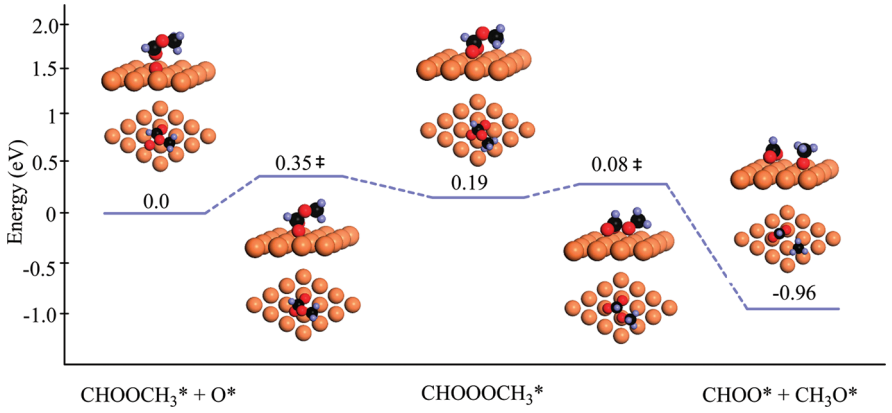

Figure 4. Energetics and geometries (top and side views) of the $CHOOCH_3^* + O^* \rightarrow CHOO^* + CH_3O^*$ (R5-II) reaction.

and is very endothermic (ΔE = 0.86 eV). The length of the breaking C−H was found to be 1.74 Å at the transition state. After the C−H bond cleavage, the H* species moves to an hcp site, and $CHOOCH_2^*$ adsorbs in a bidentate fashion with both O and C on the top of Cu atoms.

B-9. R7: $CHOOCH_3^* \rightarrow CHOO^{**} + CH_3^*$. The direct cleavage of the ester O−C bond has an unfavorable barrier of 1.50 eV. At the transition state, the distance between C of CH_3 and oxygen is found to be 2.29 Å. After reaction, methyl is located at the hcp site, and CHOO** adsorbs with each oxygen atom on the top of Cu.

IV. DISCUSSION

In our previous work, several pathways for MSR on Cu(111) have been proposed based on DFT calculations of several elementary steps for the formate mechanism.[31] Here, we will assume that the reaction follows the pathway that has the lowest barrier after the rate-limiting step, namely, the dioxomethylene pathway (Pathway B in ref 31 and shown in Figure 5 in green), although our results have shown that the other two pathways (Pathways A and C in ref 31) might also be viable. Pathways B and C involve the formate intermediate, thus consistent with the formate mechanism. As we discussed earlier, Pathway A is probably a minor channel and thus not included in the discussion.

To understand the mechanism of this heterogeneous catalytic reaction, we emphasize that adsorption energies of various species involved in these steps are as important as the reaction barriers, because desorption may compete with chemical reactions. In Figure 6, we thus collect all calculated reaction barriers/exothermicities of various elementary steps in our proposed mechanism along with the calculated adsorption energies. It becomes immediately clear that the first weakly adsorbed species along the MSR pathway is formaldehyde (CH_2O^*). As discussed before,[31] this well-established intermediate has four possible channels in the formate mechanism: desorption, dehydrogenation to formyl (CHO*), hydrogenation back to methoxyl (CH_3O^*), or reacts with hydroxyl (OH*) to form CH_2OOH^*, which proceeds eventually to CO_2. While not shown in Figure 6, the dehydrogenation step leading to HCO* and subsequently CO* requires a barrier of ∼0.65 eV,[20] and thus is not competitive with desorption. It should be noted that the DFT adsorption energy (E_{ads} = 0.06 eV) for formaldehyde is likely an underestimate because of the inability of the conventional DFT in describing van der Waals interactions,[47] but CH_2O^* is known to be a weak adsorber on copper.[18] The barrier for hydrogenation back to methoxyl is 0.21 eV, which is lower than that of dehydrogenation, but still significantly higher than the reaction with hydroxyl, which has a low barrier (0.11 eV) and large exothermicity (−0.46 eV). In addition, this hydrogenation reaction is not expected to be favorable kinetically given the large concentration of CH_3OH in the reactor. As a result, the only reaction channel that can compete effectively with formaldehyde desorption is its reaction with OH*. The further reactions from CH_2OOH^* to CO_2 can have two alternative pathways, as shown in Figure 6, but neither has a higher barrier than the rate-limiting step of dehydrogenation of methoxyl, which has a barrier of 1.12 eV.

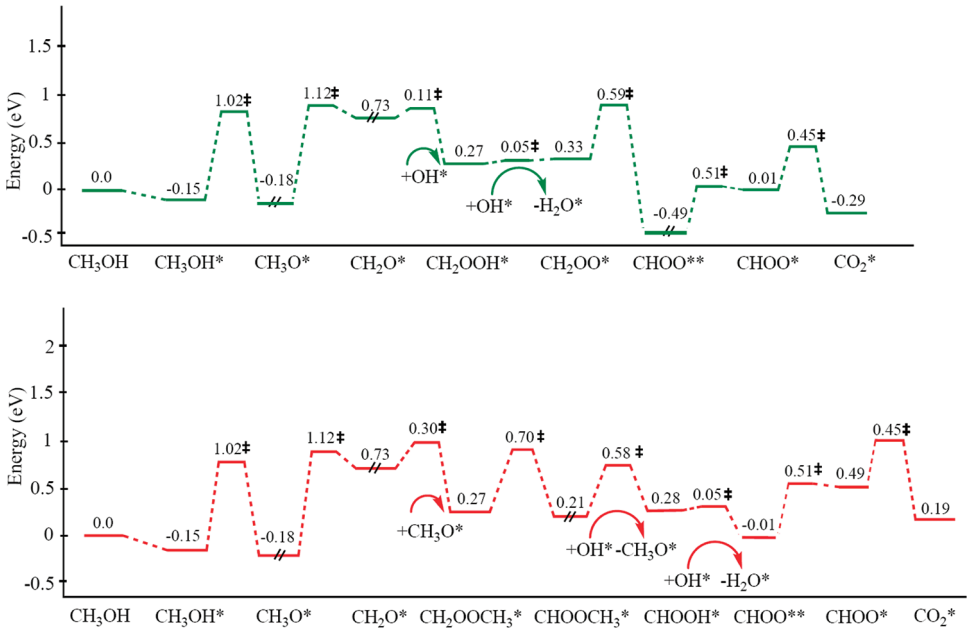

Figure 5. Energetics of the formate and methyl formate pathways for MSR. The // symbol denotes that an H* species is removed from the next step of the calculation, while the symbol ‡ indicates the barrier height in the forward direction. In the methyl formate pathway, the barrier for the $CHOOCH_3^*$ + OH* step is chosen from the first reaction (R4-IIa) since that for R4-IIc is smaller, and a relatively stable intermediate exists between the two steps (see Figure 3).

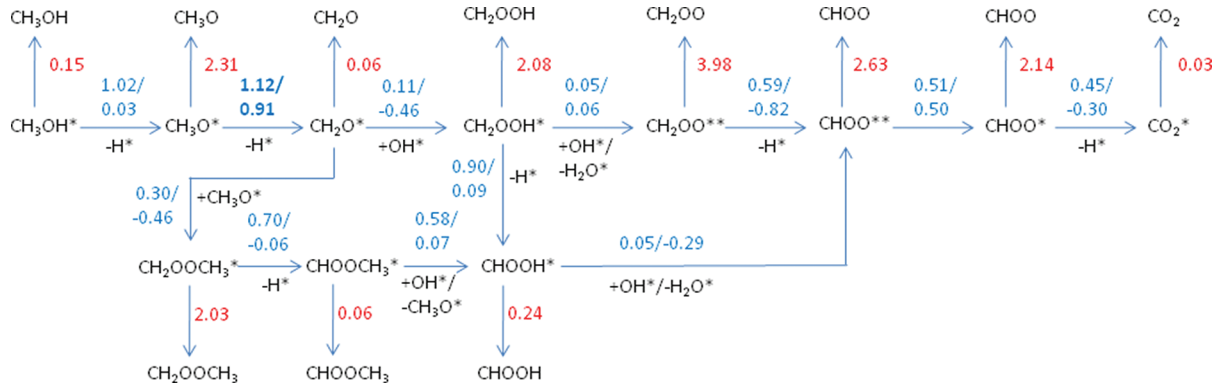

Figure 6. Network of reactions involving the formate and methyl formate pathways of MSR. The adsorption energies are colored red, while the barrier heights/exothermicities in blue. The numbers for the rate limiting step are in bold.

It is clear from our results reported here that the surface methyl formate ($CHOOCH_3^*$) species can be formed by reacting formaldehyde with methoxyl (R1), much the same way as the reaction between formaldehyde and hydroxyl. (Although it is possible for methyl formate to form by dimerization of formaldehyde (the Tischenko reaction), this channel was not considered as it not supported by experimental evidence.[18]) The reaction R1 is likely to be followed by direct dehydrogenation of $CH_2OOCH_3^*$ (R2), rather than hydrogen abstraction reaction by OH* (R3) because the latter has a much higher barrier. This observation is consistent with our earlier work, in which it was shown that OH* is much better in abstracting H from an OH group than from a CH group.[31]

In the presence of water (and thus OH*), the reaction of formaldehyde with hydroxyl is favored over the reaction with methoxyl because of its lower barrier (0.11 vs 0.30 eV). This is thus consistent with the observations that methyl formate is only produced in the absence or at low concentrations of water.[10,15,16] Under such circumstances, R1 becomes viable since the barrier is not particularly high. On the other hand, the activated nature of the reaction is also consistent with the experimental observation that methyl formate formation diminishes at low temperatures.[10]

Like formaldehyde, methyl formate is a closed-shell molecule and has a small adsorption energy on Cu. We have investigated several possible reactions for this species. First, we examined its reaction with a hydroxyl species on the surface to produce methanol and formate (R4), which can then dehydrogenate to produce the final CO_2 product. This reaction, which has been proposed by several authors,[6,7,9,11] has two possible reaction schemes. The OH* attack at the methyl carbon of methyl formate (R4-I) results in a barrier of 1.84 eV, which is unlikely to be feasible under MSR conditions. However, the attack at the carbonyl carbon leads to a metastable intermediate, $CHOOHOCH_3^*$, which undergoes a change of its adsorption configuration and then decays to CHOOH* and CH_3O^*, as denoted in Table 2 as R4-IIa,

dx.doi.org/10.1021/cs200311t |ACS Catal. 2011, 1, 1263–1271

b,c. The barrier for the first step is 0.58 eV, while the last barrier is 0.42 eV. The formic acid (CHOOH*) can further react to produce formate (CHOO**), which adsorbs in a bidentate fashion. As shown in our earlier work,[31] it has to be converted to a unidentate adsorbate (CHOO*) before decomposing to CO_2*. The CHOO* species is metastable, so the overall barrier for the conversion of CHOO** to CO_2* is 0.95 eV. Interestingly, Grabow and Mavrikakis did not find a stable CHOO* species on Cu(111), but their barrier height for the conversion is similar to ours.[34]

The second reaction (R5) we examined involves methyl formate with the more reactive O* species. This reaction also has two possible schemes. The attack of O* at the methyl carbon (R5-I) leads to a very high barrier (2.01 eV), while its attack at the carbonyl carbon (R5-II) has a much lower barrier (0.38 eV). The latter reaction is consistent with the experimental observation that methyl formate readily decomposes on O-predosed copper surfaces.[18] The barrier height is also in agreement with the recent theoretical result of Grabow and Mavrikakis.[34] However, the relevance of this process in MSR depends on the availability of the O* species, which is believed to be a minor species because of the high energy costs to produce it from H_2O.[31]

Two more reactions (R6 and R7) have been examined, both involving the decomposition of methyl formate. These processes were found to possess high barriers, as shown in Table 2. These results are consistent with the experimental observation that methyl formate is nonreactive on clean copper surfaces.[18]

In summary, five possible reaction channels, including R4, R5, R6, R7, and -R2, have been examined for the methyl formate species. Neither of these channels except R5 has a barrier that is comparable to the adsorption energy of methyl formate, which is likely a value between 0.06 eV based on our theoretical calculation and 0.41 eV from monolayer experimental TPD data.[18] As mentioned above, R5 is not expected to be a major channel because of the small population of O*. Consequently, it is highly likely that once formed, methyl formate will desorb, rather than react. This is in sharp contrast with the dioxomethylene pathway (Pathway B in ref 31), in which none of the intermediates is physisorbed on Cu(111), and the reaction to $CO_2 + H_2$ can proceed without significant loss of the flux. Even in Pathway C in ref 31, the weakly adsorbed formic acid reacts with OH* exothermically with a tiny barrier, which allows it to compete effectively with the desorption of CHOOH*. These scenarios are depicted in Figure 6.

It is, however, possible for excess methyl formate to react with surface OH* species to produce the $CO_2 + H_2$ products. The highest barrier for this process is 0.95 eV for the conversion of HCOO** to CO_2* + H*, which is still lower than that of the rate limiting step (1.12 eV). This explains the experimental observation that steam reforming of methyl formate reacts faster than MSR,[15] as the latter has to overcome the rate-limiting step of methoxyl dehydrogenation.

Our results are also illuminating in explaining the isotope exchange experiment of Papavasiliou et al.,[17] who observed $CH_3{}^{18}OH$ in the MSR process with $CH_3{}^{16}OH/H_2{}^{18}O$. These authors concluded that methyl formate has to be involved in MSR because ^{18}O from water is present in the methanol product. Their proposed pathway can be depicted as follows (the heavier oxygen (^{18}O) in italic form): $CH_2O^* + CH_3O^* \rightarrow CH_2OOCH_3^* \rightarrow CHOOCH_3^*$, followed by $CHOOCH_3 + OH^* \rightarrow CHOO^* + CH_3OH^*$. However, our results on R4 have shown that the *OH** attack at the methyl carbon of methyl formate is unfeasible because of its high barrier. On the other hand, the low-barrier *OH** attack on carbonyl carbon does not lead to the observed isotope exchange because the heavy *O* will be in CHO*O**. Thus, the isotope exchange observed by these authors cannot be explained by the formation of methyl formate. In fact, the heavy oxygen methanol can be formed without resorting to methyl formate. For example, one can imagine a scenario depicted below: $CH_2O^* + OH^* \rightarrow CH_2OOH^* \rightarrow CH_2OO^{**} \rightarrow CH_2OOH^* \rightarrow CH_2O^* (+ OH^*) \rightarrow CH_3O^* \rightarrow CH_3OH^*$. This isotope scrambling process relies on the equivalency of the two oxygen atoms in dioxomethylene, CH_2OO^{**}. Indeed, the aforementioned route has no excessive barrier, thus offering an explanation of the experimental findings. As a result, we conclude that the isotope experiment does not support the methyl formate pathway.

An important caveat is offered here concerning the reaction mechanism discussed above. It may be risky to conclude the mechanistic pathways based on the reaction barrier/exothermicity alone. A more reliable approach is to simulate MSR under appropriate reaction conditions, using for instance the kinetic Monte Carlo method. As a result, the arguments presented above should be considered qualitative, and simulations of the kinetics are underway in our laboratories.

V. CONCLUSIONS

In this DFT study, we examined the relevance of the putative methyl formate pathway in MSR that has been discussed extensively in the literature. Building on our previous work, which examined the formate pathway,[31] our theoretical studies suggests that the methyl formate is an intermediate in MSR of minor importance. Indeed, it can be formed when there are insufficient hydroxyl species on the surface. However, further reactions of methyl formate with the OH* species were found to have higher barriers than desorption. Consequently, this physisorbed species is most likely to desorb rather than react once formed because of its small adsorption energy.

The DFT results found the reaction of formaldehyde with OH* has a lower barrier than its reaction with methoxyl, thus providing an explanation of the methyl formate formation in the absence of water. Our results further explained the observation that the steam reforming of methyl formate is faster than MSR, as the former avoids the rate-limiting step for methoxyl dehydrogenation. An alternative explanation is also offered for the observed production of $CH_3{}^{18}OH$ from MSR with $CH_3{}^{16}OH/H_2{}^{18}O$ without invoking the intermediacy of methyl formate. In summary, our theoretical model is consistent with all experimental observations for MSR on copper catalysts and assigns a minor role for methyl formate in MSR.

■ ASSOCIATED CONTENT

Supporting Information. Cartesian coordinates of all computed stationary points for the reaction steps studied here. This material is available free of charge via the Internet at http://pubs.acs.org.

■ AUTHOR INFORMATION

Corresponding Author

*E-mail: dqxie@nju.edu.cn (D.X.), hguo@unm.edu (H.G.).

Present Addresses

[§]Research Institute of Photocatalysis, State Key Laboratory Breeding Base of Photocatalysis, Fuzhou University, Fuzhou 350002, China

Funding Sources

This work was supported by National Natural Science Foundation of China (20725312 and 91021010 to D.X.), by Chinese Ministry of Science and Technology (2007CB815201 to D.X.), by a New Direction grant from the Petroleum Research Fund administered by the American Chemical Society (48797-ND6 to H.G.), and by U.S. National Science Foundation (CHE-0910828 to H.G.).

■ ACKNOWLEDGMENT

We thank Manos Mavrikakis and Lars Grabow for discussing issues related to MSR and methanol synthesis.

■ REFERENCES

(1) Olah, G. A. *Catal. Lett.* **2004**, *93*, 1.
(2) Trimm, D. L.; Onsan, Z. I. *Catal. Today* **2001**, *43*, 31.
(3) Brown, L. F. *Int. J. Hydrogen Energy.* **2001**, *26*, 381.
(4) Palo, D. R.; Dagle, R. A.; Holladay, J. D. *Chem. Rev.* **2007**, *107*, 3992.
(5) Sa, S.; Silva, H.; Brandao, L.; Sousa, J. M.; Mendes, A. *Appl. Catal., B* **2010**, *99*, 43.
(6) Jiang, C. J.; Trimm, D. L.; Wainwright, M. S.; Cant, N. W. *App. Catal., A* **1993**, *93*, 245.
(7) Peppley, B. A.; Amphlett, J. C.; Kearns, L. M.; Mann, R. F. *App. Catal., A* **1999**, *179*, 31.
(8) Lee, J. K.; Ko, J. B.; Kim, D. H. *Appl. Catal., A* **2004**, *278*, 25.
(9) Frank, B.; Jentoft, F. C.; Soerijanto, H.; Krohnert, J.; Schlogl, R.; Schomacker, R. *J. Catal.* **2007**, *246*, 177.
(10) Takezawa, N.; Iwasa, N. *Catal. Today* **1997**, *36*, 45.
(11) Takahashi, K.; Kobayashi, H.; Takezawa, N. *Chem. Lett.* **1985**, 759.
(12) Wachs, I. E.; Madix, R. J. *J. Catal.* **1978**, *53*, 208.
(13) Bowker, M.; Madix, R. J. *Surf. Sci.* **1980**, *95*, 190.
(14) Fisher, I. A.; Bell, A. T. *J. Catal.* **1999**, *184*, 357.
(15) Takahashi, K.; Takezawa, N.; Kobayashi, H. *Appl. Catal.* **1982**, *2*, 363.
(16) Choi, Y.; Stenger, H. G. *Appl. Catal., B* **2002**, *38*, 259.
(17) Papavasiliou, J.; Avgouropoulos, G.; Ioannides, T. *Appl. Catal., B* **2009**, *88*, 490.
(18) Sexton, B. A.; Hughes, A. E.; Avery, N. R. *Surf. Sci.* **1985**, *155*, 366.
(19) Greeley, J.; Norskov, J. K.; Mavrikakis, M. *Annu. Rev. Phys. Chem.* **2002**, *53*, 319.
(20) Greeley, J.; Mavrikakis, M. *J. Catal.* **2002**, *208*, 291.
(21) Chen, Z.-X.; Neyman, K. M.; Lim, K. H.; Rosch, N. *Langmuir* **2004**, *20*, 8068.
(22) Sakong, S.; Gross, A. *J. Catal.* **2005**, *231*, 420.
(23) Lim, K. H.; Chen, Z.-X.; Neyman, K. M.; Rosch, N. *J. Phys. Chem. B* **2006**, *110*, 14890.
(24) Sakong, S.; Gross, A. *J. Phys. Chem. A* **2007**, *111*, 8814.
(25) Tang, Q.-L.; Chen, Z.-X. *J. Chem. Phys.* **2007**, *127*, 104707.
(26) Tang, Q.-L.; Chen, Z.-X. *Surf. Sci.* **2007**, *601*, 954.
(27) Tang, Q.-L.; Chen, Z.-X.; He, X. *Surf. Sci.* **2009**, *603*, 2138.
(28) Mei, D. H.; Xu, L. J.; Henkelman, G. *J. Phys. Chem. C* **2009**, *113*, 4522.
(29) Gu, X.-K.; Li, W.-X. *J. Phys. Chem. C* **2010**, *114*, 21539.
(30) Bo, J.-Y.; Zhang, S.; Lim, K. W. *Catal. Lett.* **2009**, *129*, 444.
(31) Lin, S.; Johnson, R. S.; Smith, G. K.; Xie, D.; Guo, H. *Phys. Chem. Chem. Phys.* **2011**, *13*, 9622.
(32) Mei, D.; Xu, L.; Henkelman, G. *J. Catal.* **2008**, *258*, 44.
(33) Yang, Y.; Evans, J.; Rodriguez, J. A.; White, M. G.; Liu, P. *Phys. Chem. Chem. Phys.* **2010**, *12*, 9099.
(34) Grabow, L. S.; Mavrikakis, M. *ACS Catal.* **2011**, *1*, 365.
(35) Kresse, G.; Hafner, J. *Phys. Rev. B* **1993**, *47*, 558.
(36) Kresse, G.; Furthmuller, J. *Phys. Rev. B* **1996**, *54*, 11169.
(37) Kresse, G.; Furthmuller, J. *Comput. Mater. Sci.* **1996**, *6*, 15.
(38) Perdew, J. P.; Chevary, J. A.; Vosko, S. H.; Jackson, K. A.; Pederson, M. R.; Singh, D. J.; Fiolhais, C. *Phys. Rev. B* **1992**, *46*, 6671.
(39) Blochl, P. *Phys. Rev. B* **1994**, *50*, 17953.
(40) Kresse, G.; Joubert, D. *Phys. Rev. B* **1999**, *59*, 1758.
(41) Monkhorst, H. J.; Pack, J. D. *Phys. Rev.* **1976**, *B13*, 5188.
(42) Methfessel, M.; Paxton, A. T. *Phys. Rev. B* **1989**, *40*, 3616.
(43) *CRC Handbook of Chemistry and Physics*; CRC Press: New York, 1996.
(44) Jonsson, H.; Mills, G.; Jacobsen, K. W. In *Classical and Quantum Dynamics in Condensed Phase Simulations*; Berne, B. J., Ciccotti, G., Coker, D. F., Eds.; World Scientific: Singapore, 1998.
(45) Henkelman, G.; Jonsson, H. *J. Chem. Phys.* **2000**, *113*, 9978.
(46) Gokhale, A. A.; Dumesic, J. A.; Mavrikakis, M. *J. Am. Chem. Soc.* **2008**, *130*, 1402.
(47) Sauer, J.; Ugliengo, P.; Garrone, E.; Saunders, V. P. *Chem. Rev.* **1994**, *94*, 2095.
(48) Redhead, P. A. *Can. J. Phys.* **1964**, *42*, 886.
(49) Millar, G. J.; Rochester, C. H.; Waugh, K. C. *J. Chem. Soc., Faraday Trans.* **1991**, *87*, 2785.